Proceedings of the IASS 2024 Symposium
Redefining the Art of Structural Design
August 26-30, 2024, Zurich, Switzerland
Philippe Block, Giulia Boller, Catherine DeWolf,
Jacqueline Pauli, Walter Kaufmann (eds.)

Multistable Polyhedral Origami Modules for Curved Surface Assembly

Munkyun LEE[a], Kiumars SHARIFMOGHADDAM[b], Tomohiro TACHI[*]

[*] Department of General System Studies, Graduate School of Arts and Sciences, The University of Tokyo
153-8902, Building 15-702, 3-8-1 Komaba, Meguro-ku, Tokyo, Japan
tachi@idea.c.u-tokyo.ac.jp

[a] Department of Architecture, Graduate School of Engineering, The University of Tokyo
[b]Institute of Discrete Mathematics and Geometry & Center for Geometry and Computational Design, TU Wien

Abstract

Multistable origami that can transform between flat and deployed states and maintain its stability at the deployed states holds possibilities for civil and architectural applications. In this paper, we propose a novel modular system for building curved surfaces by assembling multistable origami modules. Drawing inspiration from T-hedral tubes, we design the 1-degree-of-freedom flat and rigidly foldable polyhedra with symmetrical convex polygonal trajectories. By connecting already coinciding open ends, we induce panel deformation during deployment, thus imparting multistability. Using this method, we design various multistable origami modules such as triangular, quadrilateral, pentagonal, and hexagonal trajectories, validating multistability through bar-and-hinge analysis and physical prototypes. We assemble these modules to realize planar, cylindrical, dome, and extended surfaces. We also demonstrate that some complex structures can be entirely folded into a flat state depending on assembly methods.

Keywords: Multistable origami, Deployable structure, Modular system, Metamaterial, Discrete shell, Tessellation, Computational geometry, Lightweight structure, Structural morphology

1. Introduction

Origami has become a source of inspiration for transformable and deployable structures due to its stackable storage, reusability, and lightweight benefits. In architecture and civil engineering, because these benefits can help to reduce the carbon footprint during transportation and construction, and lower waste through reuse or replacement, the origami-inspired deployable structure can be a suitable solution for a new sustainable building system [1, 2, 3, 4, 5].

Among deployable origami structures, there are two distinctive types. A popular approach is to use *rigid-foldable origami*, a transformable structure in which rigid panels are connected by rotational joints. Rigid foldable origami can deploy from the folded state to the deployed state without distortion of the panels [6]. They have advantages in the ability to be built from thick panels and be used in any of the continuous families of folded configurations. However, maintaining the stability (or fixing) of the deployed state is a challenging engineering issue when applying complex geometric patterns of origami to large-scale structures. *Multistable origami*, in contrast, induces elastic deformation of panels during the deployment process and exhibits energy stability at more than one configuration. Multistable origami has the potential to maintain its stability in the deployed state in use [7]. However, their application to architectural surfaces such as domes or curved roofs was limited.

In this study, we explore the potential of multistable origami and its shape stability to be used for the construction of curved surfaces. In particular, we propose a novel construction method for planar, cylindrical, and dome-like surfaces using multistable origami as the assemblage modules.

1.1. Background

Among well-known multistable origami patterns, there are multiple examples such as the Kresling pattern [8], square-twist folding pattern [9], and origami hypar [10] being capable of maintaining multiple specific shapes and exhibits snap-through behavior when transitioning between these shapes. This unique property has garnered interest from scientists and engineers across various fields, showcasing its potential for engineering applications such as tactile feedback [11], isolators [12], mechanical memory [13], and more. Most of these applications are designed by assembling known multistable origami as the building block. As such building blocks have predefined manners, it is difficult to design the desired stable shapes of assembled structures.

To solve this design issue, analytical design methods based on rigid-foldable origami have been proposed. Melancon et al. [7] proposed a *geometrical incompatibility design method* that joins multiple rigid-foldable origami modules with incompatible deployment paths to induce panel deformations. Also, Lee et al. [14] designed multistable origami using the incompatibility between the linkage structure and rigid origami modules and showed that their stiffness can be tunable. Kamrava et al. [15] proposed a *closed-loop design method* that imparts multistability by designing a rigid-foldable origami strip and connecting both ends to create a loop. These methods allowed users to design multistable structures with specific stable shapes, such as arch and tent-like structures [7]. However, knowledge about achievable shapes like three-dimensional curved surfaces remains limited.

1.2. Objective

This paper proposes a novel modular building system that constructs curved surfaces by assembling multistable origami modules. We (1) design multistable origami modules based on the rigidly foldable tubes called T-hedral tubes [16] and (2) investigate achievable curved surfaces by tessellating the designed modules. Our modular system can be a new perspective on transformable and sustainable building construction methods with potential applications in emergency housing, temporary structures, and lightweight spatial structures, emphasizing reusability.

In Section 2, we describe the design method of multistable origami modules based on these T-hedral tubes. In Section 3, we validate the multistability through the simulation and prototype hands-on interaction test. In Section 4, we assemble the designed modules and realize various surfaces. In Section 5, we conclude this paper.

2. Module Design

We propose a novel method, called *T-toroidalization*, for creating multistable modules based on closing rigidly foldable tubes into toroids. In particular, we design six types of representative multistable modules with symmetric convex polygonal trajectories. The structures have valid flat-folded states and deployed states.

2.1. Construction of T-hedral tube

We first construct rigidly foldable tubes using the concept of Trapezoidal polyhedra (T-hedra), which are a special type of planar quad (PQ) meshes with rigid faces, valence-four vertices, and rotational

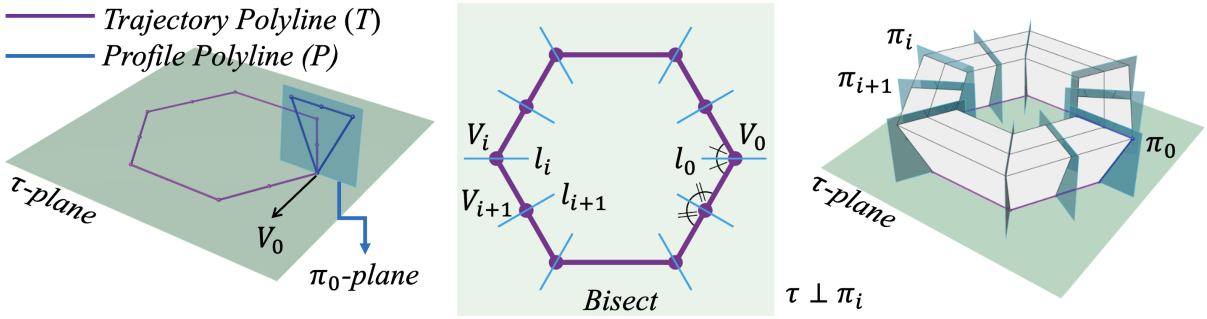

Figure 1: Design process of T-hedral tube(T-tube).

joints on their edges. While such PQ meshes are usually geometrically rigid, T-hedral structures exhibit a 1-Degree-of-Freedom (DoF) deformation, preserving the rigidity of the planar faces [17].

A T-hedron can be constructed using two planar boundary polylines, referred to as *profile* and *trajectory* polylines (denoted as P and T respectively), lying on two perpendicular planes (π_0 and τ) that share a vertex V_0, along with a series of profile planes (π_i, $i = 0, \ldots, k$) perpendicular to τ (see Figure 1). Each profile plane π_i can be determined by l_i, the intersection line of π_i with τ, and passes through the corresponding vertex V_i of the trajectory polyline. The construction is straightforward, involving the projection of P along T onto the π_i-planes and the subsequent connection of corresponding vertices at each projection step.

A cylindrical topology, called T-hedral tube (T-tube), can be achieved by utilizing a closed polygon P as the profile. While we anticipate the resulting tube to exhibit rigidity, preserving the 1-DoF movement is contingent upon satisfying the loop closure condition outlined in Theorem 3.1 of [16].

2.2. Closing the Module

To obtain a module, we construct a toroidal mesh by using a closed trajectory and stitching the two end profile curves. To get closure at the deployed state, (1) the profile polygons at the start and the end need to be congruent. In addition, to have the flat-folded state, we impose the condition of flat-foldability. Flat foldability is achieved by making (2) the T-tube (before ends are connected) flat-foldable and (3) the trajectory polygon flat-folded to a line. Condition (2) is achieved by positioning π_i-planes to bisect each segment angle around V_i, thus endowing the structure with flat-foldability [16]. Conditions (1) and (3) are achieved by using symmetric trajectory polylines.

2.3. Design Variations

As representative modules, we design various T-hedral toroids (T-toroids) with triangular, quadrilateral, pentagonal, and hexagonal trajectories, and deltoidal or hexagonal profiles, to assemble standard curved surfaces (planar, cylindrical, and dome surfaces). Figure 5 illustrates these design variations with their defining lengths and angular parameters.

A T-tube with a polygonal profile reaches a flexion limit when at least one profile segment becomes parallel to τ [16]. Hence, we opt for deltoidal and hexagonal profiles, ensuring that when they reach their flexion limit in the fully deployed state, their deformed cross-sections become triangular and quadrilateral, respectively. Modifying the parameters l, r, and α can control the overall shape of a tessellated curved surface. For example, the values in Figure 5 yield the shapes showcased in Section 4..

To make the flat-foldable trajectory, we split the trajectory polygon at the midpoints of its segments.

Without these additional joints (blue circled purple points on the trajectory polyline in Figure 5), the trajectory curve will fold with a total turn angle of $n\pi$, where n is the number of vertices of the polygon. To make the total turn into 2π, $n-2$ additional joints are added, each of which turns by $-\pi$. Thus, we have installed the $n-2$ joints at the appropriate positions to enable flat-foldability.

2.4. Multistability

While the designed T-tubes with ends not connected are rigid-foldable, their rigid motion does not preserve their topology, as the trajectories open up and often impose self-intersections during the motion (see the rigid folding motion part of Figure 5).

We obtain T-toroids, the toroidal topology modules with multistability, by hinge-connecting and closing at both end cross-sections of designed T-tubes. Geometrically, the structure is rigid and valid in the deployed and flat-folded states. In actual material, the structure has no strain in the flat-folded and deployed states. The motion between these states induces deformation in panels upon deployment, thereby generating the strain energy barrier and the snap-through behavior.

3. Evaluation of Multistability

Here, we evaluate the multistability of T-toroids through the bar-and-hinge simulation and hands-on interaction test of physical prototypes.

3.1. Bar-and-Hinge Analysis

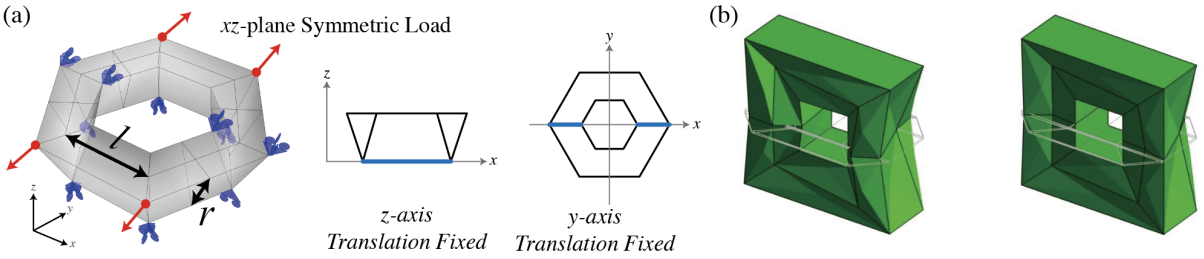

Figure 2: (a) The boundary conditions of the bar-and-hinge simulation. The bottom of the structure is z-translation fixed, and the surfaces on xz-plane are y-translation fixed. Loading direction is xz-plane symmetric. (b) The local buckling motion of the Quad-Hexagon module.

We implemented the bar-and-hinge model [18] in MATLAB using Merlin2 software [19] to validate the multistability. Figure 2(a) shows the boundary condition settings. We set constraints to allow the structure to deform symmetrically. The modules are positioned to be symmetric about the xz-plane. Vertices on the xz-plane have y-axis translation fixed, while vertices on the bottom have z-axis translation fixed. We apply forced displacement to the upper vertices of the outmost panels with no midpoint joints symmetrically with respect to xz-plane. The loading starts from the flat state and deforms to the fully deployed state. In this analysis, we consider only the panel stiffness represented by bar elements and the angular spring within each panel. We neglect the hinge stiffness between panels or other unexpected behaviors like local buckling. To achieve this model, we chose the material parameters of the bar-and-hinge analysis as follows: Young's modulus (E^*) and Poisson ratio of the panel are set to 100 and 0.25, respectively, and the Length scale factor (L^*) is set to $10,000$ [14]; also to prevent the local buckling problem by the panel twist, we use a sufficiently rigid panel by setting the panel thickness to 1.

Figure 6 plots the energy with respect to the deployment rate (top) and the load with respect to the deployment rate (bottom) obtained from this analysis. The deployment rate is calculated as 100% at the second stable position. Strain energy is the total energy of panel bending and bar stretch energies and the load indicates the average reaction forces of y-direction loading points. The multistable motion in Figure 5 shows the deformation aspects of modules during the analysis.

From Figure 6, we can confirm that all modules show bistability, which has stable flat and deployed states and snap-through behavior between these states. Also, we can capture some unexpected behaviors from the Pentagon and Quad-Hexagon modules. In the energy-deployment plot of the Pentagon module, the second energy minimum is not 0. This is because the value of the forced displacement differs from the front and back parts, interrupting simultaneous snap-through. It can be observed in Figure 5 that the back part of the pentagon module snapped through first, and then the front part snapped through(fourth and fifth images from the left of multistable motion). At this time, the load on the back part continued until the front part was deployed, resulting in strain energy, not 0. Another unexpected behavior is observed in the load-deployment plot of the Quad-Hexagon module. This occurs from the local buckling in the panels when the energy drops from the maximum point. This local buckling affects the reaction force of each load point, so the load-displacement plot shows unstable results. Figure 2 (b) displays the local buckling motions at the moment between the fourth and fifth multistable motions of the Quad-Hexagon module in Figure 5.

3.2. Prototypes

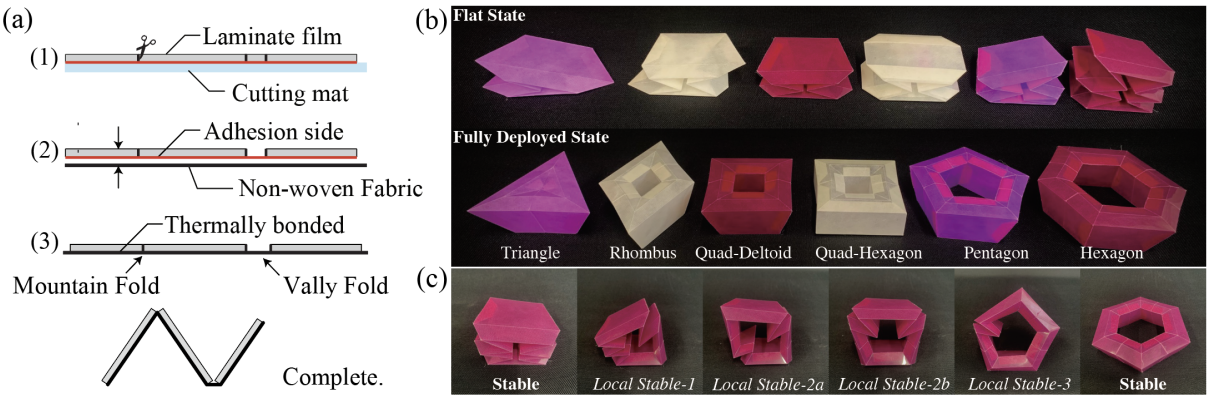

Figure 3: (a) Process of the fabrication. (b) Pictures of flat and fully deployed states of fabricated prototypes. (c) Stable and local stable states of the Hexagon module. It also shows the sequence of deploying and folding processes.

We fabricated physical prototypes of the designed modules to validate the multistability. We used a $0.25\,\mathrm{mm}$ thick heat-bonded laminate film as the material for the panels and employed nonwoven fabric as hinges to minimize hinge stiffness. The fabrication process is as follows [14]:
(1) the pattern is cut into a laminate film using a cutting plotter, inserting a single-line cut on mountain folds and a $0.7\,\mathrm{mm}$ wide cut on valley folds; (2) the engraved laminate film is transferred on the non-woven fabric, with the adhesive side facing toward the nonwoven fabric; (3) two layers are thermally bonded using an iron, and the unnecessary materials are trimmed off; and (4) the necessary parts are adhered to each other with double-sided tape.

Figure 3(b) shows flat and fully deployed states of physical prototypes. We deployed the flat modules by pulling each midpoint joint part outward and folded the deployed modules by pushing each midpoint

joint part inward (see Figure 3 (c)). Through hands-on interaction tests, we experienced multistability in all modules. In the actual behavior, between the designed two stable states of completely flat and deployed, we found multiple local stable states, where each midpoint joint is individually deployed, as shown in Figure 3 (c). In addition, some modules exhibit asymmetric stiffness properties. For example, the Hexagon and Quad-Deltoid modules with the boundary conditions shown in Figure 2(a) are relatively flexible in the flat-to-deployment direction. In contrast, it is stiffer in the opposite (deployment-to-flat) direction. This indicates that some modules are locked at the fully deployed state and can act as an ideal static building block.

4. Curved Surface Assembly

Using the designed modules, we constructed a variety of curved surfaces. To assemble standard curved surfaces, we considered the geometric conditions for the T-toroids to be tessellated face-to-face without gaps. Moreover, we show that more extended curved surfaces can be obtained by loosening the assembly rules.

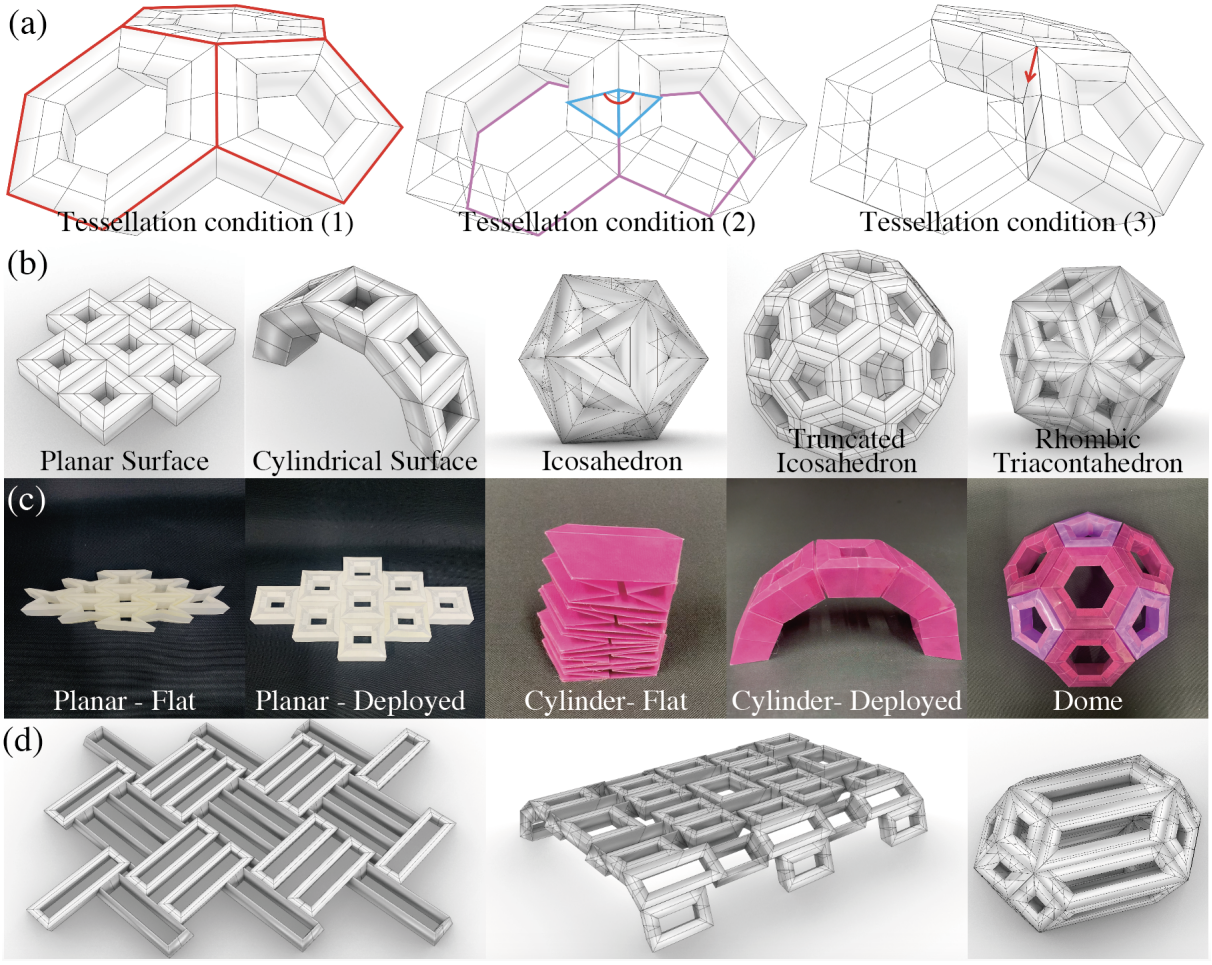

Figure 4: (a) Tessellation conditions with the truncated icoshedron example. Red lines indicate the outermost trajectories. Blue and purple polylines indicate profile and trajectory polylines respectively. The red arrow indicates the shared common vector between neighboring modules. (b) computer graphics, and (c) physical prototypes of the assembled standard curved surfaces. planar and cylindrical surfaces can be globally flat-foldable. (d) computer graphics of extended curved surfaces.

4.1. Tessellation Conditions

Flat-foldable T-toroids obtained by our method maintain the same cross-section along the trajectory. Therefore, the overall shape of the block is frustum constructed by extruding a polygon with a constant taper. When bonding two T-toroids together, the tapered sides meet face-to-face, and the dihedral angle between polygons is formed as the summation of the tapers of two modules. This assembly rule enforces the constraints on the target surface shape that can be achieved (Figure 4 (a)). For a polyhedral surface to be assembled by the module, (1) the outermost trajectory of the T-toroid needs to match the polygon of the surface; (2) the dihedral exterior angle of an edge shared by two faces equals the sum of taper angles of the corresponding modules; and (3) for each vertex, there is a shared common vector between the tapered sides of shared frusta. The last condition enforces the complete closure of the module at the vertex; however, this may not be required for some applications.

4.2. Assembly Results

Figure 4 (b) and (c) show computer graphics and physical prototypes of assembled standard curved surfaces, such as planar-, cylindrical-, and dome types. They follow conditions (1), (2), and (3) by having the consistent taper angles. In the physical prototypes, we connected each module using double-sided tapes.

For the planar surface, we used Quad-Hexagon modules forming prisms with no taper and assembled them in the stretcher-bonding pattern in a constant direction. This assembly is globally flat-foldable, i.e., the module can be flat-foldable in the assembled state. The global structure deploys well in one direction by pulling the structure in both sides of the horizontal direction in the picture, while folding from the deployed state to the flat state requires compressing each module separately.

For the cylindrical surface, we assemble Quad-Deltoid modules in a row. However, this cannot be straightforwardly tessellated in the transverse direction since the taper starts to form curvature in this direction as well leading to a double-curved surface. The structure is globally flat-foldable but is stiff enough to sustain its cylindrical shape in the fully deployed state.

We can achieve dome surfaces using various tessellation methods. Figure 4(b) shows an icosahedron using Triangular modules, a truncated icosahedron using Pentagon and Hexagon modules, and a rhombic triacontahedron using Rhombus modules. While these structures don't exhibit global flat-foldability, each module prevents compressing each other, so modules function as an ideal static building block. Therefore, these structures can take advantage of load-bearing capacity. It is also stiff in the prototype(Figure 4(c) Dome) and was able to support vertical load 39.9 times its weight ($71.9\,\mathrm{g}$).

Furthermore, we expect that there are more possible tessellation patterns beyond these examples, such as regular polyhedra (Platon solids), some semi-regular polyhedra (Archemidian solids, prisms), rhombus-based Catalan solids, and other isohedra may be possible using our module design.

4.3. Extended Curved Surface

To design various curved surfaces, we give design flexibility to the trajectory and profile polyline by stretching or shortening the designed modules. Also, we removed condition (3) and allowed the modules to alternate their orientation to control the entire curvature. Figure 4 (d) shows the extended planar, cylindrical, and dome-type curved surface with flipping module assembly.

The planar surface shows a basket weave tiling method employing solely Rectangular modules with tapers. Although it loses global flat-foldability, the pattern appears more aesthetically than the Quad-Hexagon assembly. Furthermore, each module acts like an ideal static building block, so the structure

is expected to be stiffer in the assembled state. The extended cylindrical surface consists of three types of rectangular modules, including the ones used to form the planar surface. Modules can be added or removed in horizontal or vertical directions as much as the designer wants. The whole structure is still globally flat-foldable, but all modules are not connected. The capsule-type curved surface is constructed by stretching the rhombic triacontahedron model. We believe other more complex curved surfaces and assembly methods can be designed beyond these examples.

5. Conclusion and Future works

We have designed multistable origami modules with symmetric convex polygonal trajectories based on the T-tube and validated multistability through the bar-and-hinge simulation and physical prototypes. We have realized various curved surfaces by tessellating modules and showed that certain surfaces could achieve global flat-foldability depending on the assembly method.

The entire geometric space of multistable T-toroidal modules and other generalizations of flat-foldable non-rigid origami tori have yet to be explored. In the next steps of our research, we plan to investigate these theoretical aspects and explore various complex curved surfaces as well. Ultimately, we aim to construct large-scale prototypes. We will integrate compliant hinges [20] to enable folding deformation in thicker materials, control the stiffness of both modules and assembled structures, and analyze the load-bearing behaviors of the designed modules to develop a more reliable modular system. Additionally, we are considering introducing an air pressure system to make the entire structure operational.

Acknowledgments

This work is supported by JST AdCORP "Realization of people- and environment-friendly artifacts by leveraging computational design and fabrication." The first author was supported by JSPS 24KJ0648. The second author was supported by Austrian Science Fund (FWF) project F 77 (SFB "Advanced Computational Design")

References

[1] T.-U. Lee and J. M. Gattas, "Geometric design and construction of structurally stabilized accordion shelters," *Journal of Mechanisms and Robotics*, vol. 8, no. 3, p. 031 009, 2016.

[2] J. Gattas and Z. You, "Design and digital fabrication of folded sandwich structures," *Automation in Construction*, vol. 63, pp. 79–87, 2016.

[3] K. Ando *et al.*, "Lightweight rigidly foldable canopy using composite materials," *SN Applied Sciences*, vol. 2, pp. 1–15, 2020.

[4] R. Maleczek, K. Sharifmoghaddam, G. Nawratil, and C. Preisinger, "Bridging the gap–a study on foldable tubular bridges," in *Proceedings of IASS Annual Symposia*, International Association for Shell and Spatial Structures (IASS), vol. 2023, 2023, pp. 1–11.

[5] Y. Zhu and E. T. Filipov, "Large-scale modular and uniformly thick origami-inspired adaptable and load-carrying structures," *Nature Communications*, vol. 15, no. 1, p. 2353, 2024.

[6] T. Tachi, "Simulation of rigid origami," *Origami*, vol. 4, no. 08, pp. 175–187, 2009.

[7] D. Melancon, B. Gorissen, C. J. García-Mora, C. Hoberman, and K. Bertoldi, "Multistable inflatable origami structures at the metre scale," *Nature*, vol. 592, no. 7855, pp. 545–550, 2021.

[8] C. Jianguo, D. Xiaowei, Z. Ya, F. Jian, and T. Yongming, "Bistable behavior of the cylindrical origami structure with kresling pattern," *Journal of Mechanical Design*, vol. 137, no. 6, p. 061 406, 2015.

[9] J. L. Silverberg *et al.*, "Origami structures with a critical transition to bistability arising from hidden degrees of freedom," *Nature materials*, vol. 14, no. 4, pp. 389–393, 2015.

[10] E. Filipov and M. Redoutey, "Mechanical characteristics of the bistable origami hypar," *Extreme Mechanics Letters*, vol. 25, pp. 16–26, 2018.

[11] Z. Chang *et al.*, "Kirigami haptic swatches: Design methods for cut-and-fold haptic feedback mechanisms," in *Proceedings of the 2020 CHI Conference on Human Factors in Computing Systems*, 2020, pp. 1–12.

[12] S. Ishida, K. Suzuki, and H. Shimosaka, "Design and experimental analysis of origami-inspired vibration isolator with quasi-zero-stiffness characteristic," *Journal of Vibration and Acoustics*, vol. 139, no. 5, p. 051 004, 2017.

[13] H. Yasuda, T. Tachi, M. Lee, and J. Yang, "Origami-based tunable truss structures for non-volatile mechanical memory operation," *Nature communications*, vol. 8, no. 1, p. 962, 2017.

[14] M. Lee, Y. Miyajima, and T. Tachi, "Designing and analyzing multistable mechanisms using quadrilateral boundary rigid origami," *Journal of Mechanisms and Robotics*, vol. 16, no. 1, p. 011 008, 2024.

[15] S. Kamrava, R. Ghosh, Z. Wang, and A. Vaziri, "Origami-inspired cellular metamaterial with anisotropic multi-stability," *Advanced Engineering Materials*, vol. 21, no. 2, p. 1 800 895, 2019.

[16] K. Sharifmoghaddam, R. Maleczek, and G. Nawratil, "Generalizing rigid-foldable tubular structures of t-hedral type," *Mechanics Research Communications*, p. 104 151, 2023.

[17] K. Sharifmoghaddam, G. Nawratil, A. Rasoulzadeh, and J. Tervooren, "Using flexible trapezoidal quad-surfaces for transformable design," in *Proceedings of IASS Annual Symposia*, International Association for Shell and Spatial Structures (IASS), vol. 2020, 2020, pp. 1–13.

[18] E. Filipov, K. Liu, T. Tachi, M. Schenk, and G. H. Paulino, "Bar and hinge models for scalable analysis of origami," *International Journal of Solids and Structures*, vol. 124, pp. 26–45, 2017.

[19] K. Liu and G. Paulino, "Highly efficient nonlinear structural analysis of origami assemblages using the merlin2 software," *Origami*, vol. 7, pp. 1167–1182, 2018.

[20] M. LEE and T. TACHI, "Design and evaluation of compliant hinges for deployable thick origami structures," in *Proceedings of IASS Annual Symposia*, International Association for Shell and Spatial Structures (IASS), vol. 2023, 2023, pp. 1–11.

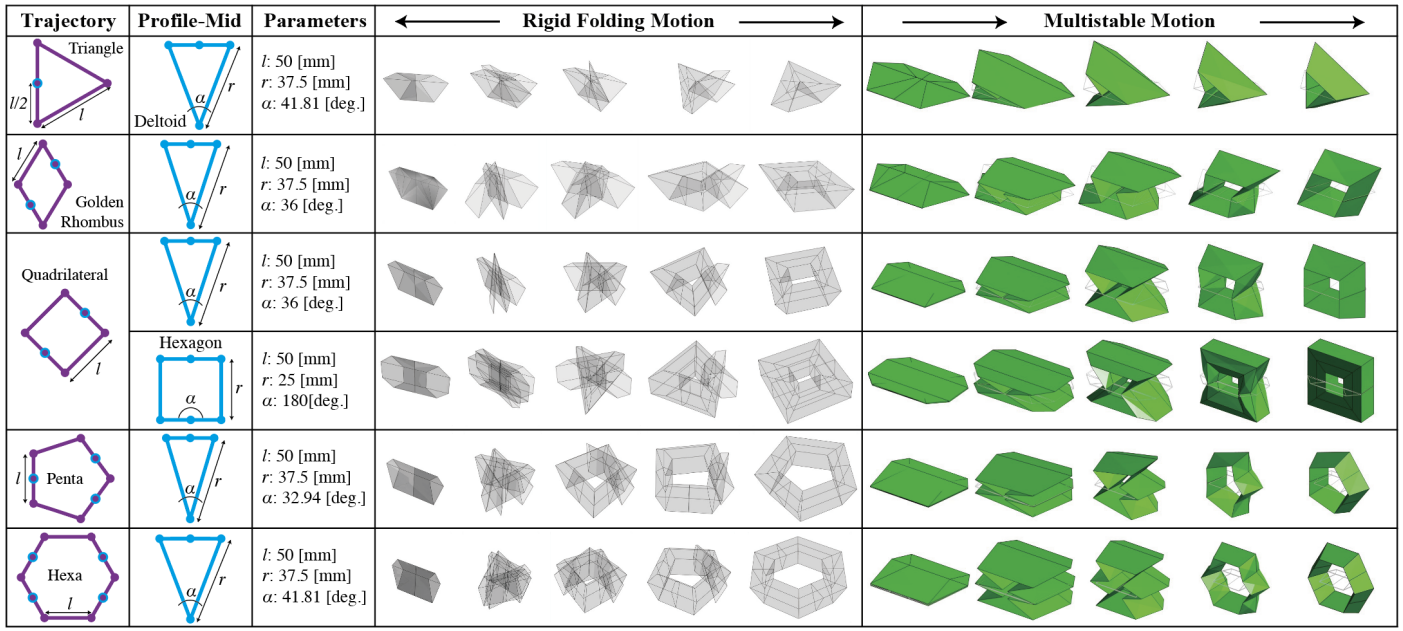

Figure 5: Design parameters and rigid folding motion of the designed T-tubes and multistable motion of the designed T-toroids. Points on the trajectory and profile polygons represent rotational joints. Profile-Mids indicate profile polygons at the midpoint joint(blue-circled purple points) of trajectory segments.

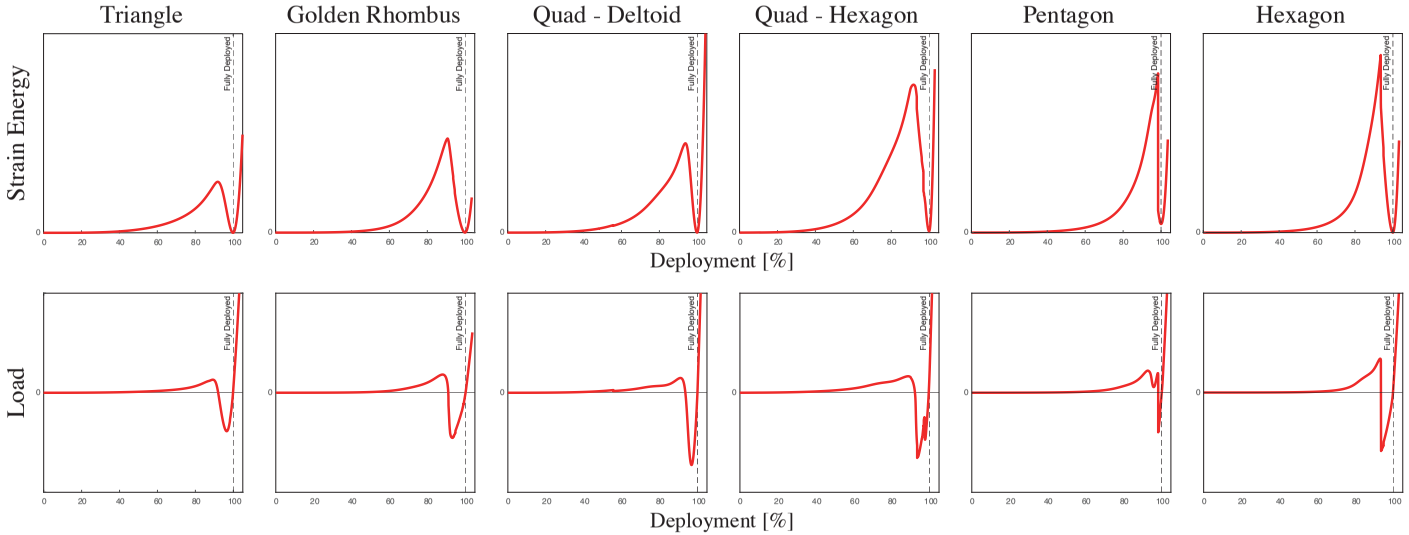

Figure 6: Results of the bar-and-hinge analysis. The upper plots are strain energy-deployment plots and the lower plots are load-deployment plots.